PERGAMON

International Journal of Heat and Mass Transfer 43 (2000) 2931–2948

International Journal of HEAT and MASS TRANSFER

www.elsevier.com/locate/ijhmt

A lumped parameter model of the operating limits of one-well geothermal plant with down hole heat exchangers

Alberto Carotenuto[a,*], Claudio Casarosa[b]

[a]Dipartimento di Ingegneria Industriale, Università degli Studi di Cassino, via Di Biasio 43, 03043 Cassino, Italy
[b]Dipartimento di Energetica, Università degli Studi di Pisa, Pisa, Italy

Received 8 February 1999; received in revised form 4 October 1999

Abstract

In one-well geothermal plant, the mass flow of the geothermal fluid between the aquifer and the heat exchanger is supplied only by one well. It is universally acknowledged that this type of plant has some thermal and fluid dynamic limits and, therefore, they were proposed only for low and medium thermal applications; however simple models are lacking to explain and correctly evaluate these limits. The fundamentals of a lumped parameter model of the thermal and fluid dynamic phenomena giving rise to heat flow limits were explained by Carotenuto et al. (A. Carotenuto, C. Casarosa, M. Dell'Isola, L. Martorano, An aquifer–well thermal and fluid dynamic model for downhole heat exchangers with a natural convection promoter, Int. J. Heat Mass Transfer 40(18) (1997) 4461–4472; A. Carotenuto, C. Casarosa, Modello a Parametri Concentrati dei Limiti Operativi di Impianti Geotermici a Pozzo Unico. Parte I: Elementi Generali, 53°Congresso Nazionale ATI, Firenze, vol. I, 1998, pp. 557–570). In this paper, the model is completely developed for natural convection plant in which the geothermal fluid flow between aquifer and well is provided only by the temperature drop occurring in the heat exchanger. The model is applied to this type of plant taking into consideration, whether: (i) a natural convection promoter is present and (ii) downhole heat exchangers or geothermal convectors (GTCs) are used. In particular, for GTCs, the model is successfully applied to evaluate the experimental data obtained by the authors in previous experimental tests.

1. Introduction

Fundamentals of a lumped parameter model, developed to describe the interaction between aquifer and well of a geothermal plant in which heat transfer occurs only by natural convection, are reported in [1,2]. In the present paper, the model is completely formulated taking into account all the parts of the plant. Infact, even though the model is simplified by the assumption of lumped parameters, it needs the entire plant and particularly the heat exchanger to be completely characterized. Hence, in the present paper the authors have studied natural convection plant distinguishing between plant with a downhole heat exchanger (DHE) [3] and plant with a geothermal convector (GTC) [4], i.e. a special geothermal application of the two-phase thermosyphon. In particular, it consists of a sealed vessel partially filled with a working fluid. At the bottom, the working fluid evaporates, the vapour rises to the top where it condenses, and it transfers heat flow to the fluid of the user plant, then the condensate returns by gravity to the evaporation section.

* Corresponding author.

0017-9310/00/$ - see front matter
PII: S0017-9310(99)00361-0

Nomenclature

b	coefficient of σ rational equation
c	specific heat at constant pressure (kJ/kg K)
k_0, k_1	circulation coefficients (kW/K^2)
m	parameter defined by Eq. (14b)
N	transfer unit number defined by Eq. (27)
n	parameter defined by Eqs. (6a) and (6b)
U	overall heat transfer coefficient (kW/m^2 K)
R	thermal resistance of the adiabatic section (K/kW)
R_0, R_1, R_2	parameter defined by Eq. (39) (K/kW^2; K/kW^3)
S	heat exchanger surface (m^2)
T	temperature (K)

Greek symbols

γ	dimensionless heat capacity rate of the cooling fluid in the user plant
ε	heat exchanger effectiveness
μ	coefficient of σ exponential equation
η	effectiveness of system defined by Eq. (4)
θ	dimensionless temperature difference defined by Eq. (5)
λ	adiabatic section parameter defined by Eq. (42a)
λ_0, λ_1, λ_2	adiabatic section parameters defined by Eq. (42b)
ξ	aquifer dimensionless heat capacity rate defined by Eq. (3)
ρ	circulation ratio defined by Eq. (13)
σ	short-circuit ratio defined by Eq. (1)
χ	dimensionless heat flow defined by Eq. (3)
ω	well mean temperature thermal weighting parameter

Superscripts and subscripts

a	mass transfer between aquifer and well
a1, a2	renewed geothermal fluid
con	condenser
e	external environment
ev	evaporator
f	geothermal fluid crossing through heat exchanger
h	heat exchanger
i	inlet
max	maximum
o	outlet
th	thermodynamic limit
u	user plant cooling fluid
w	geothermal fluid circulating between aquifer and well
∞	unperturbed geothermal fluid

Moreover, the model introduces a distinction between plant with a single and double convection loop. In the first case, the geothermal fluid, circulating between the aquifer and the well, crosses through the heat exchanger inserted in the well; in the second case, the plant has a device, known as the convection promoter, that gives rise inside the well to a second loop of natural convection to be added to the one already established between aquifer and well [5]. Finally, dimensionless form of the model is used to process and analyze the experimental results obtained from the natural convection plant realised by the authors.

2. General introduction to the model

In the lumped parameter model presented in [1,2], the thermal and fluid dynamic fields induced between the well and the geothermal aquifer, were modelled through the short-circuit ratio σ, for both, forced and natural convection:

$$\sigma = \frac{T_\infty - T_{wi}}{T_\infty - T_{wo}} \tag{1}$$

where T_∞ is the geothermal fluid temperature in unperturbed conditions and T_{wi} and T_{wo} are the mean inlet and outlet temperatures of the geothermal fluid in the well, respectively. This parameter represents the part of the mass flow rate circulating between aquifer and well that is short-circuited between the well slotted casing outlet and inlet [1,2,6]. Consequently, the fluid mean temperature at the slotted casing inlet is less than that of the renewed geothermal fluid in unperturbed conditions, $T_{wi} < T_\infty$ [1,6]. From Eq. (1) the heat flow, $\dot{Q}$, of the plant as a function of the mass flow rate of geothermal fluid circulating between well and aquifer, $\dot{m}_a$, can be evaluated as:

$$\dot{Q} = \dot{m}_a c_a (1 - \sigma)(T_\infty - T_{wo}) \tag{2}$$

where c_a is the specific heat of the geothermal fluid. Generally, the short-circuit ratio depends on many variables, but one of the basic hypothesis of the proposed model assumes that only the dependence on the geothermal fluid flow $\dot{m}_a$ is significant. This hypothesis

is verified using numerical simulations of aquifer–well system, moreover, for a natural convection plant characterized by $0 < \dot{m}_a < 4000$ kg h^{-1}, these simulations have shown that $\sigma(\dot{m}_a)$ function is well interpolated using both rational ($\sigma = \frac{b(c_a\dot{m}_a)^n}{1+b(c_a\dot{m}_a)^n}$) or exponential ($\sigma = 1 - \exp(-\mu(c_a\dot{m}_a)^n)$) functions [1,2,6], where the exponent n is in the range $1 < n \leq 3$ for the rational function and $0 < n \leq 3$ for the exponential function.

If the rational or exponential short-circuit function is assigned, and the thermodynamic limit condition is assumed to be the geothermal fluid cooled up to the external environment temperature T_e, then the heat flow of the plant $\dot{Q}$, can show a maximum value for specific values of the heat capacity rate ($c_a\dot{m}_a$), and the short-circuit ratio σ, both of which are completely defined by the parameters characterizing the short-circuit function [6]. In order to render the model equations in a dimensionless form, the maximum heat flow, $\dot{Q}_{max}$, and the corresponding values of $(c_a\dot{m}_a)_{max}$ and σ_{max} were used in Ref. [6] and the dimensionless heat capacity rate, ξ, and the dimensionless heat flow χ were introduced:

$$\begin{cases} \xi = \dfrac{c_a\dot{m}_a}{(c_a\dot{m}_a)_{max}} \\ \chi = \dfrac{\dot{Q}}{\dot{Q}_{max}} \end{cases} \tag{3}$$

Moreover, the system effectiveness η and the dimensionless temperature difference θ were also introduced:

$$\eta = \frac{T_\infty - T_{wo}}{T_\infty - T_{ui}} \tag{4}$$

$$\theta = \frac{T_\infty - T_{ui}}{T_\infty - T_e} \tag{5}$$

where η is defined as the ratio between the temperature drop of the renewed geothermal fluid and the operating temperature difference of the plant (T_{ui} is mean inlet cooling temperature, see Fig. 8), while θ is defined as the ratio between the aforesaid operating temperature difference and the maximum one available in the system. The dimensionless forms for the rational and exponential short circuit functions are, respectively:

$$\sigma = \frac{\xi^n}{n - 1 + \xi^n} \quad \text{with } n > 1 \tag{6a}$$

$$\sigma = 1 - \exp\left(-\frac{\xi^n}{n}\right) \tag{6b}$$

and for the dimensionless heat flow we obtain:

$$\chi = \frac{1-\sigma}{1-\sigma_{max}}\eta\theta\xi \tag{7}$$

where, for rational short circuit factor

$$\sigma_{max} = \frac{1}{n} \tag{8a}$$

and for exponential short circuit factor

$$\sigma_{max} = 1 - \exp(-1/n) \tag{8b}$$

In natural convection plant, the fluid circulation is induced by cooling of the geothermal fluid in the heat exchanger inserted in the well: in particular, the flow is driven by the fluid density gradients and, therefore, it is connected with the difference between the aquifer fluid temperature and the one inside the well. The mass flow rate of the circulating fluid between aquifer and well and the one that crosses the heat exchanger in the well, are not necessarily equal. This depends on the presence of a convection promoter in the well [3,4]. The use of this device depends on the aquifer characteristics. In particular, plant without a promoter can be proposed for very thick aquifers in the order of magnitude of 10 m as in the layout shown in Fig. 1(a). Plant with a promoter can be proposed for aquifers of contained thickness in the order of magnitude of meters as in the layout shown in Fig. 1(b).

In the absence of a promoter, the above-mentioned mass flow rates of the fluid are equal (see Fig. 1a) and the plant can be classified as "single convection loop plant". Whereas, in plant with a promoter installed in the well, the circulating mass flow rate in the heat exchanger is generally different from the one that circulates between the aquifer and the well (see Fig. 1b), and in this case, the plant is defined as "double convection loop plant". In both these cases, the heat capacity rate of geothermal fluid circulating between the aquifer and the well can be evaluated as:

$$c_a\dot{m}_a = k_0(T_\infty - T_{wm}) \tag{9}$$

Eq. (9) is obtained from the momentum balance in the hypothesis of laminar flow both, in the aquifer and the well. The circulation coefficient k_0 takes into account the dependence on geometrical and physical characteristics of the aquifer and the well, whereas the temperature T_{wm} is the mean weighted temperature inside the well. This temperature can be expressed by a "thermal weighting" parameter as linearly dependent on the well inlet and outlet temperatures of the geothermal fluid:

$$T_{wm} = T_{wo} + \omega(T_{wi} - T_{wo}) \tag{10}$$

where ω (lying in the range $0 \leq \omega \leq 1$) is the above-mentioned parameter that depends on the well characteristics, the position and geometry of the heat ex-

changer and, in particular, on the presence of a convection promoter. From the definition (1) of the short circuit ratio and from Eqs. (9) and (10), we obtain:

$$c_a\dot{m}_a = \left[1-\omega(1-\sigma)\right]k_0(T_\infty - T_{wo}) \tag{11}$$

and using Eq. (2) it is possible to obtain:

$$\dot{Q} = \frac{\dfrac{(c_a\dot{m}_a)^2}{k_0}}{\dfrac{1}{1-\sigma}-\omega} \tag{12}$$

Eqs. (11) and (12) are fundamental for the analysis of natural convection plants. In the case of plant without a promoter, see Fig. 1(a), the mass flow rate of geothermal fluid circulating between the aquifer and the well is the same crossing through the heat exchanger. Moreover, the parameter ω depends on the geometry of the system but can be considered independent of the mass flow rate of the circulating fluid. When the heat exchanger is much shorter than the aquifer thickness, it is reasonable to suppose a ω value close to 0 if the heat exchanger is placed at the top of the well casing near the geothermal fluid inlet section. On the contrary, ω assumes a value close to 1, if the heat exchanger is placed at the bottom of the well tube near the fluid outlet section. If the heat exchanger has a length comparable with that of the slotted section of the tube casing, then an ω value near to 1/2 can be expected as is usual for heat exchangers with low temperature differences between the inlet and outlet section. With the hypothesis of ω independent of the mass flow rate, single loop plant can be analyzed using Eqs. (11) and (12). In order to complete the model, it is necessary to add the relationship characterizing the heat exchanger.

Eqs. (11) and (12) are not sufficient to describe the convection phenomena for the double loop plant, because the dependence of ω on the mass flow rate cannot be neglected in the presence of the convection promoter. For a layout as shown in Fig. 1(b), the mass flow rate of the fluid circulating between aquifer and well, $\dot{m}_a$, and the fluid circulating inside the well-promoter-heat exchanger system, $\dot{m}_f$, are not the same; the parameter ω is a function of the ratio ρ defined as the circulation ratio [1]:

$$\rho = \frac{\dot{m}_a}{\dot{m}_f} \tag{13}$$

Since, as shown in Fig. 2, two different conditions can be delineated, the first in which $\dot{m}_f$ is greater than $\dot{m}_a$ (low value of ρ) and the second in which, vice versa, $\dot{m}_a$ is greater than $\dot{m}_f$ (high value of ρ), then the following dependence of ω on ρ can be assumed:

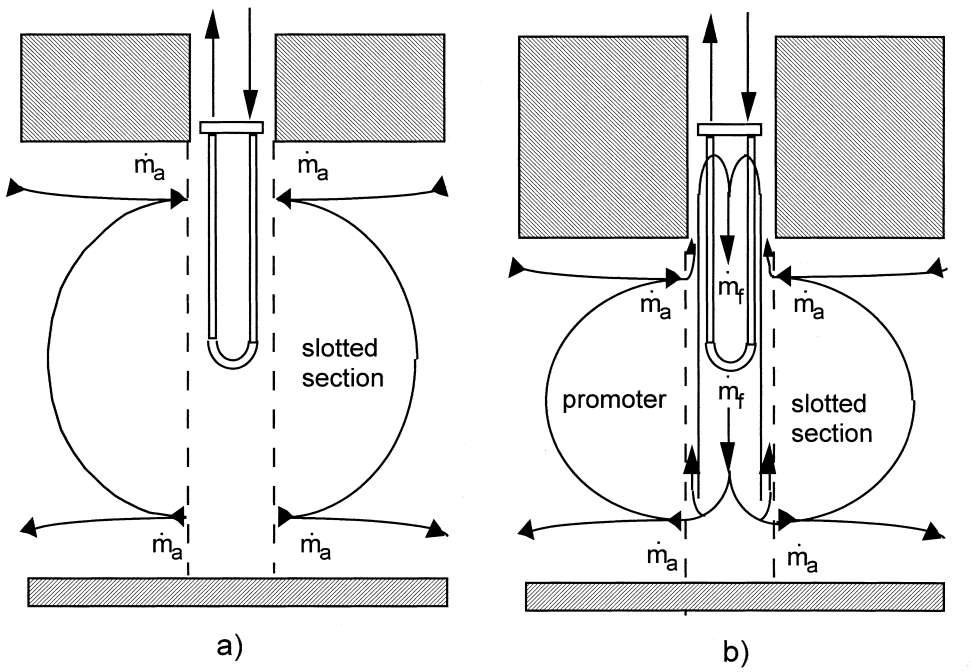

Fig. 1. Layout of the natural convection for geothermal plant with only well. (a) Single loop convection without convection promoter; (b) double loop convection with convection promoter.

$$\omega = f(\rho) \quad \text{with} \begin{cases} \omega \cong 0 & \text{for } 0 \le \rho \ll 1 \\ \omega = \dfrac{1}{2} & \text{for } \rho = 1 \\ \omega \cong 1 & \text{for } \rho \gg 1 \\ \dfrac{d\omega}{d\rho} \ge 0 & \text{for } \rho \ne 1 \end{cases} \tag{14a}$$

One of the possible functions with these properties is the rational one, with a real positive exponent m:

$$\omega = \frac{\rho^m}{1+\rho^m} \tag{14b}$$

where the exponent is related to the mixing between the renewed geothermal fluid from the aquifer and the circulating fluid into the well; low values of m are typical of efficient mixing, vice versa, high values characterize weak mixing. Some experimental temperature trends in the well suggested weak mixing occurs, showing that the influence of the renewed geothermal fluid can be felt exclusively in the final part of the slotted section of the tube casing [4,9]. Therefore in similar conditions, high value of m are to be expected, at a first approximation a discontinuous "step" function can also be accepted for the properties defined by Eq. (14a) (zero values for $\rho < 1$, unitary values for $\rho > 1$ and values equal to 1/2 for $\rho = 1$).

As regards the heat capacity rate of the geothermal fluid circulating in the convection promoter and crossing through the heat exchanger, in the hypothesis of laminar flow, it is possible to obtain an equation similar to (9), as a function of the difference between the mean temperatures of the warm and cold fluid circulating in the promoter. In order to avoid further complications of the lumped parameters model, these temperatures can be considered as equal to the inlet T_{hi} and outlet T_{ho} temperatures from the heat exchanger, thereby obtaining:

$$c_f \dot{m}_f = k_1 (T_{hi} - T_{ho}) \tag{15}$$

The circulation coefficient k_1 takes into account the dependence on geometrical characteristic of the well, type of heat exchanger and presence of natural convection promoter.

Then, the energy balance furnishes:

$$\dot{Q} = c_f \dot{m}_f (T_{hi} - T_{ho}) \tag{16}$$

and finally:

$$\dot{Q} = \frac{(c_f \dot{m}_f)^2}{k_1} \tag{17}$$

For a double convection loop plant Eqs. (11) and (12) have to be completed with Eqs. (15) and (17) using the functional link defined in Eq. (14a). We must then add to these equations the ones relating to the type of heat exchanger, as reported for the single convection loop and the forced convection plant.

To generalize the problem, it is useful to give dimensionless form of the natural convection plant equations dimensionless. It is evident that the heat capacity rate of natural geothermal fluid circulating between aquifer and well, for the maximum temperature difference of the plant, presents a thermodynamic limit equal to:

$$(c_a \dot{m}_a)_{th} = k_0 (T_\infty - T_e) \Longrightarrow \xi_{th} = \frac{(c_a \dot{m}_a)_{th}}{(c_a \dot{m}_a)_{max}} \tag{18}$$

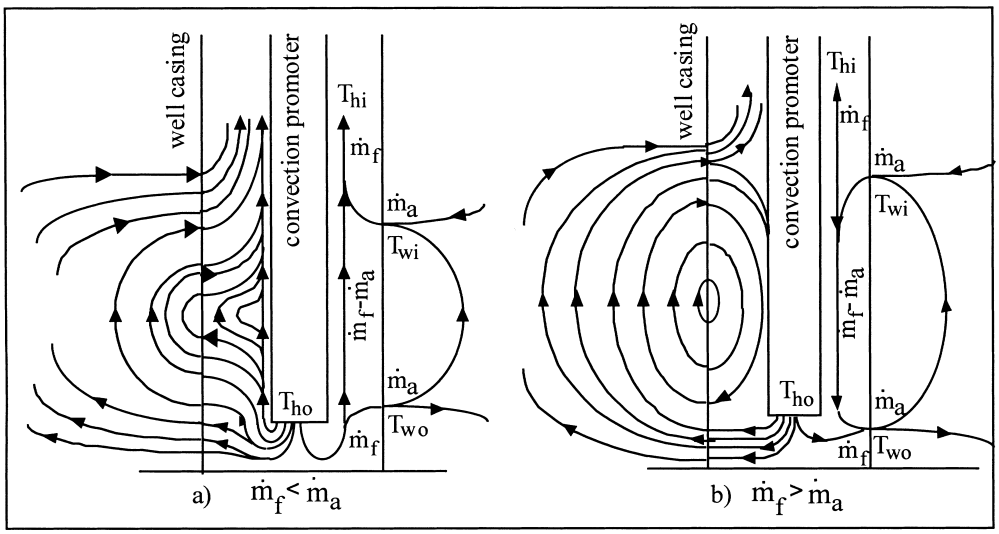

Fig. 2. Sketch of the fluid dynamic field for double loop natural convection. (a) Circulation ratio $\rho \le 1$; (b) circulation ratio $\rho \ge 1$.

The dimensionless value ξ_{th}, is always positive, and can be lesser or greater than 1, but however, it represents the upper bound of the allowable interval of the dimensionless heat capacity rate ξ. By substituting in Eq. (11), the parameters defined in Eqs. (4) and (5), and by considering Eqs. (3) and (18), we can easily obtain:

$$\xi = \xi_{th} \cdot \left[1 - \omega(1-\sigma)\right]\eta\theta \tag{19}$$

and, finally, using Eq. (12) we will have obtained the dimensionless heat flow:

$$\chi = \frac{(1-\sigma)\left(\xi^2/\xi_{th}\right)}{(1-\sigma_{max})\left[1-\omega(1-\sigma)\right]} \tag{20}$$

Although $\sigma(\xi)$ is an assigned function, Eqs. (19) and (20) are not sufficient to complete the lumped parameter model of the plant, even in the case of the single convection loop model in which ω is a constant. In fact, Eq. (19) can furnish the function $\xi(\theta)$, and, therefore $\chi[\xi(\theta)]$, only when both the effectiveness η and the function $\sigma(\xi)$ are known. Generally, η is a function of ξ by means of the short circuit ratio and of several more parameters characterizing the heat exchanger performances. A detailed analysis of the heat exchangers is therefore absolutely necessary. We can note, finally, that even if ω is a parameter as in the single convection loop, the dimensionless heat flow χ given by Eq. (20) does not necessarily increase for $\omega \rightarrow 1$, because ξ is a decreasing function of ω, as shown in Eq. (19).

For double loop plant, where ω is a function of the circulation ratio ρ, Eq. (20) is coupled to Eq. (17), rearranged in a dimensionless form:

$$\chi = \frac{\left(\xi^2/\xi_{th}\right)}{(1-\sigma_{max})(k_1/k_0)\rho^2} \tag{21}$$

From Eqs. (20) and (21) the following is obtained:

$$\frac{k_1}{k_0}\rho^2 + \omega(\rho) = \frac{1}{1-\sigma(\xi)} \tag{22}$$

This non linear equation furnishes the function $\rho(\xi)$ [2].

To complete the natural convection model and then to evaluate the heat flow function $\chi(\theta)$, the model is simplified by introducing the hypothesis of negligible heat losses in the well and the heat exchanger plant. This hypothesis could be removed producing a model with unchanged outline, but still further complicated. Moreover, on the basis of the experimental results [4,9], the aforesaid hypothesis is quite plausible. Consequently, the geothermal heat flow is wholly transferred to the user cooling fluid:

$$\dot{Q} = c_u \dot{m}_u (T_{uo} - T_{ui}) \tag{23}$$

where T_{uo} is its mean outlet cooling temperatures (see Fig. 8).

Furthermore, the distinction between single and double loop convection was introduced. In single convection plant, the whole mass flow rate of geothermal fluid, circulating between aquifer and well, crosses through the heat exchanger placed in the well (a traditional heat exchanger for DHE plant or a two-phase thermosyphon evaporator for GTC plant). Due to the assumption of negligible heat losses, geothermal fluid temperatures at the heat exchanger inlet, T_{hi}, and outlet, T_{ho}, are equal to those at the well inlet, T_{wi}, and outlet, T_{wo}:

$$\begin{cases} \dot{m}_f = \dot{m}_a \Longrightarrow c_f \dot{m}_f \cong c_a \dot{m}_a \\ T_{hi} = T_{wi} \\ T_{ho} = T_{wo} \end{cases} \tag{24}$$

As clearly stated above and already shown in Fig. 2, for double loop convection plant the geothermal fluid flow circulating between aquifer and well is not the same as that crossing through the heat exchanger placed in the well. In this case, on the basis of a lumped parameter model, under the hypothesis of constant specific heat, i.e. $c_a \cong c_f$, and assuming an adiabatic mixing between the mass flow crossing through promoter and heat exchanger and the mass flow from the aquifer into the well, the following relationships can be written:

$$\text{for } \rho \leq 1 \begin{cases} T_{ho} = T_{wo} \\ T_{hi} = \rho T_{wi} + (1-\rho) T_{wo} \end{cases} \tag{25a}$$

$$\text{for } \rho \geq 1 \begin{cases} T_{hi} = T_{wi} \\ T_{ho} = \rho T_{wo} - (\rho - 1) T_{wi} \end{cases} \tag{25b}$$

In any case, to close the natural convection model it is necessary not only to distinguish between single and double loop convection, but also to evaluate the system effectiveness η depending on the type of heat exchanger and the mass flow rate of the user fluid. Thus, two types of plant are separately analyzed: (i) the general case of a usual heat exchanger placed inside the well (DHE) and (ii) the particular case of a two-phase thermosyphon with the evaporator inside the well and condenser at ground level (GTC).

3. Down-hole heat exchanger (DHE)

DHE plant exchange apparatus is a heat exchanger placed inside the well transferring the heat flow between the geothermal fluid, on one side, and the user fluid on the other. Sometimes the heat exchanger is a

tube coil and can be roughly studied as a counter-flow heat exchanger. However, the heat exchanger is usually a U tube [3,5] or even a U tube bundle that can be studied as a shell and tube exchanger with one passage of the geothermal fluid, on the shell side, and two or more passages of the cooling user fluid inside the tubes. To evaluate heat exchanger performance, the effectiveness ε can be introduced and two different cases can be taken into consideration as follows [7]:

$$\begin{cases} \varepsilon = \dfrac{T_{hi} - T_{ho}}{T_{hi} - T_{ui}} & \text{for} \quad c_f \dot{m}_f \le c_u \dot{m}_u \\ \varepsilon^* = \dfrac{T_{uo} - T_{ui}}{T_{hi} - T_{ui}} & \text{for} \quad c_f \dot{m}_f \ge c_u \dot{m}_u \end{cases} \tag{26a}$$

Taking into account the energy balance of the heat exchanger, we obtain:

$$\varepsilon^* = \frac{c_f \dot{m}_f}{c_u \dot{m}_u} \varepsilon \tag{26b}$$

The effectiveness is usually formulated as a function of dimensionless parameters [7]; in particular, it is useful to express heat exchanger effectiveness by means of the following parameters:

$$\begin{cases} N = \dfrac{US}{(c_a \dot{m}_a)_{max}} \\ g = \dfrac{c_u \dot{m}_u}{(c_a \dot{m}_a)_{max}} \end{cases} \tag{27}$$

where N is the number of transfer units, γ the dimensionless heat capacity rate of the cooling fluid, S the heat exchanger surface and U the overall heat transfer coefficient. N and γ can be considered as parameters of the model even if the overall heat transfer coefficient U certainly depends on convective heat transfer and, therefore, is a function of the mass flow rates $\dot{m}_f$ and $\dot{m}_u$. However, taking the functional link $N(\xi, \gamma)$ into consideration only introduces a further complication but does not invalidate the model. Once the heat exchanger effectiveness is completely determined, the system effectiveness can also be calculated. It is however necessary to proceed distinctly for single and double loop convection.

3.1. DHE without convection promoter

In this case, Eq. (24) have to be applied and the effectiveness depending on the arrangement of the heat exchanger, is assigned as a known function of the type:

$$\begin{cases} \varepsilon = f(N, \gamma, \xi) \\ \varepsilon^* = \dfrac{\xi}{\gamma} \varepsilon \end{cases} \tag{28}$$

When the tube coil is assumed to be a counter-flow heat exchanger, the effectiveness ε is [7]:

$$\varepsilon = \frac{1 - \exp\left[- N\left(\xi^{-1} - \gamma^{-1}\right)\right]}{1 - \dfrac{\xi}{\gamma} \exp\left[- N\left(\xi^{-1} - \gamma^{-1}\right)\right]} \tag{29a}$$

In literature, the former equation is used only when $\xi < \gamma$, but in this instance, since:

$$\varepsilon = \frac{N}{N + \gamma} \quad \text{for } \xi \to \gamma \tag{29b}$$

it has to be considered consistent for every positive value of ξ, so that ε^* can also be determined by means of Eq. (28).

Furthermore, in the case of DHE plant with a shell and tube heat exchanger, we have [7]:

$$\varepsilon = 2 \cdot \left\{ 1 + \frac{\xi}{\gamma} + \sqrt{1 + \left(\frac{\xi}{\gamma}\right)^2} \cdot \frac{1 + \exp\left[- (N/\xi)\sqrt{1 + (\xi/\gamma)^2}\right]}{1 - \exp\left[- (N/\xi)\sqrt{1 + (\xi/\gamma)^2}\right]} \right\}^{-1} \tag{30}$$

Eqs. (1), (2), (4), (23) and (28), together with the boundary conditions (24), furnish a system of eight equations. This system is linear for the unknown quantities T_{wo}, T_{wi}, T_{ho}, T_{hi}, T_{uo}, $c_f \dot{m}_f$, η and $\dot{Q}$; these can be determined, for each mass flow rate field, as functions of (i) the temperature T_{ui} and T_∞; (ii) the heat capacity rates $c_a \dot{m}_a$ and $c_u \dot{m}_u$ and (iii) the parameters $(c_a \dot{m}_a)_{max}$, N, σ and ε. The system effectiveness for $\xi \geqslant 0$ is:

$$\eta = \frac{\varepsilon(N, \gamma, \xi)}{1 - \sigma(n, \xi)\left[1 - \varepsilon(N, \gamma, \xi)\right]} \tag{31}$$

Eq. (31) highlights the dependence of σ and ε on the other characteristic parameters of the plant. Clearly, for $\varepsilon(\xi)$, this means function (29a) or (30), extended to the positive real values of the variable ξ. However, we want to underline that, for natural convection, the variable ξ is not an independent variable, but, as can be seen from Eq. (19), is a function of the operating temperature difference in the plant and it cannot assume values greater than the thermodynamic limit defined in Eq. (18), i.e. ξ_{th}.

In order to evaluate plant performance, once Eq. (31) has been obtained, one is left only to set up a system with Eqs. (19) and (20). In these, the weighting parameter ω has to be considered as being known,

since the characteristics of the well, the geometry and the position of the heat exchanger are given. The system contains the non-linear equation (19), usually with a transcendental solution $\xi(\theta)$ that, introduced into Eq. (20), closes the problem. An easy alternative procedure is to use ξ as an intermediate variable substituting Eq. (31) in (19), and then, for values of $\xi \in [0, \xi_{th}]$, to solve the parametric equations explicitly:

$$\begin{cases} \theta = \dfrac{\xi}{\xi_{th}} \cdot \dfrac{\sigma(\xi) + \left[(1-\sigma(\xi))/\varepsilon(\xi)\right]}{1 - \omega \cdot (1-\sigma(\xi))} \\ \chi = \dfrac{(1-\sigma(\xi))\left(\xi^2/\xi_{th}\right)}{(1-\sigma_{max})\left[1-\omega(1-\sigma(\xi))\right]} \end{cases} \tag{32}$$

Obviously, the intermediate variable ξ can be removed by placing values of $\chi(\xi)$ in tables or graphs, for each value of ξ, as a function of $\theta(\xi) \in [0, 1]$. In terms of dimensionless parameters, the solution obtained gives $\xi(\theta)$ and $\chi(\theta)$, as well as, obviously, $\sigma(\theta)$ and $\varepsilon(\theta)$, as functions of (i) the short-circuit function exponent n, (ii) the number of transfer units N, referred to the heat capacity rate arising from the maximum heat flow, (iii) the cooling fluid dimensionless heat capacity rate γ, (iv) the well temperature weighting parameter ω, and (v) the thermodynamic limit of the heat capacity rate ξ_{th}.

The non-linear equations of the model are not suitable for an analytical study of the solution, and in this paper it is not the case to present an extensive numerical study of the influence of the five parameters on the solution. Figs. 3–5 show some results obtained by means of the proposed model for a DHE plant with shell and tube heat exchanger with $N = 4$, and using a rational type of short-circuit function, with $n = 3$, see Eq. (6a). The values chosen for n and N take into account the analysis of related experimental results analysis (see Section 4.2). The high value of N depends on its different definition (see Eq. (27)) with respect to the standard [7] and in particular, on low values of the $(c_a \dot{m}_a)_{max}$ as estimated for a natural convection plant [9]. In relation to the cases shown in Fig. 3, for $\gamma = 1$ and $\omega = 0$, it is possible to observe that as ξ_{th} increases, the maximum values of heat flow can move for temperature differences lower than the thermodynamic limit, i.e. for $\theta < 1$. This observation is still valid for the dimensionless user mass flow rate, i.e. γ, increasing when both, the thermodynamic limit ξ_{th} and the weighting parameter ω are assumed constant, as shown in Fig. 4 for $\xi_{th} = 3$ and $\omega = 0$. Moreover, it is easy to see that the maximum values of the dimensionless heat flow depend on ξ_{th}, but are not γ-dependent. The dependence of χ on ω is more complicated as shown by Fig. 5, which is obtained keeping constant both the dimensionless user mass flow rate and the

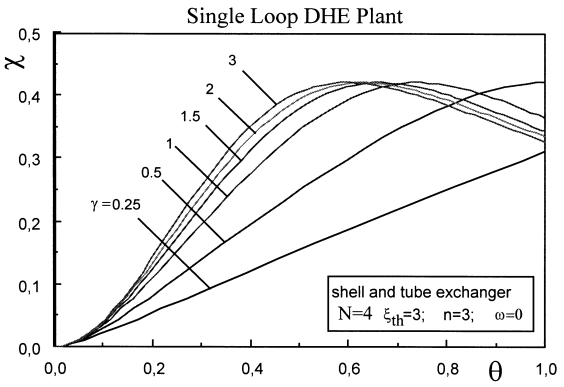

Fig. 4. Dimensionless heat flow χ vs. the dimensionless heat capacity rate of the cooling fluid γ for a DHE without convection promoter.

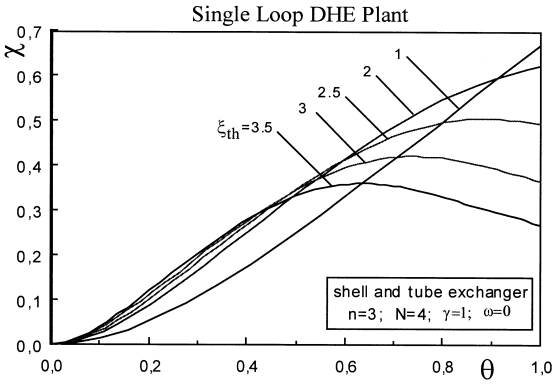

Fig. 3. Influence on the dimensionless heat flow χ of the thermodynamic limit of the dimensionless heat capacity rate ξ_{th} for a DHE without convection promoter.

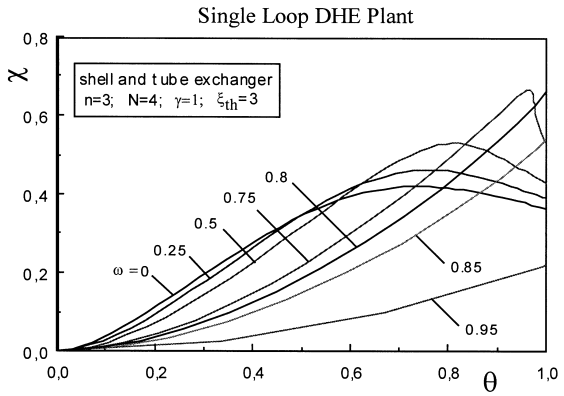

Fig. 5. Dimensionless heat flow χ vs. the weighting parameter ω for a DHE without convection promoter.

thermodynamic limit of heat capacity rate, i.e. $\gamma = 1$, and $\xi_{th} = 3$. When the weighting parameter ω rises, the maximum value of χ increases and moves towards higher values of θ, to disappear completely for values of ω close to unity, in particular, for $\omega \geq 0.8$ in the case examined.

3.2. DHE with convection promoter

In this type of plant, the mass flow rate of geothermal fluid $\dot{m}_f$, crossing through the heat exchanger, is not the same circulating between aquifer and well, $\dot{m}_a$. Consequently, the model requires the circulation ratio ρ to be introduced in addition to the dimensionless heat capacity rate ξ. Assuming the specific heat of the geothermal fluid as constant, $c_a \cong c_f$, and using the dimensionless parameters defined by Eq. (27), the heat exchanger effectiveness is a function of the type:

$$\begin{cases} \varepsilon = f(N, \gamma, \rho, \xi) \\ \varepsilon^* = \dfrac{\xi}{\gamma\rho}\varepsilon \end{cases} \tag{33}$$

that, for the counter-flow heat exchanger,

$$\varepsilon = \frac{1 - \exp\left[-N(\rho/\xi - 1/\gamma)\right]}{1 - \left[\xi/(\rho\gamma)\right] \cdot \exp\left[-N(\rho/\xi - 1/\gamma)\right]} \tag{34}$$

and for the shell and tube heat exchanger:

$$\varepsilon = 2 \cdot \left\{ 1 + \left(\frac{\xi}{\gamma\rho}\right) + \sqrt{1 + \left(\frac{\xi}{\gamma\rho}\right)^2} \cdot \frac{1 + \exp\left[-(N\rho/\xi)\sqrt{1 + \left(\xi/(\gamma\rho)\right)^2}\right]}{1 - \exp\left[-(N\rho/\xi)\sqrt{1 + \left(\xi/(\gamma\rho)\right)^2}\right]} \right\}^{-1} \tag{35}$$

Both these equations have to be extended to values of $\xi/\rho \geq \gamma$. The heat exchanger effectiveness equation (33), (34) or (35), complete the model fundamental equations, to which has to be added the functional link between the weighting parameter ω and circulation ratio ρ, as for instance occurs in Eq. (14b).

In this way, we have a non linear system of 13 equations with the same number of unknown quantities T_{wo}, T_{wi}, T_{ho}, T_{hi}, T_{uo}, $c_a\dot{m}_a$, $c_f\dot{m}_f$, ρ, σ, ε, ω, η and $\dot{Q}$, which can be determined as functions of (i) the temperatures T_{ui} and T_∞, (ii) the heat capacity rate $c_u\dot{m}_u$, (iii) the parameters $(c_a\dot{m}_a)_{max}$, n, N, k_0, k_1 and m in case of Eq. (14b).

It is worthwhile to notice that, since there are two different ranges of validity for conditions (25a) and (25b), it is also necessary in the solution to distinguish two intervals for the circulation ratio ρ. In particular, the system effectiveness η, concerning the geothermal aquifer, well and heat exchanger, proves to be:

$$\begin{cases} \eta = \dfrac{\varepsilon(\xi)}{\varepsilon(\xi) + \rho(\xi) \cdot \left[1 - \sigma(\xi)\right] \cdot \left[1 - \varepsilon(\xi)\right]} & \text{for} \quad \rho \leq 1 \\ \eta = \dfrac{\varepsilon(\xi)}{\sigma(\xi) \cdot \varepsilon(\xi) + \rho(\xi) \cdot \left[1 - \sigma(\xi)\right]} & \text{for} \quad \rho \geq 1 \end{cases} \tag{36}$$

These relationships contain the parameters σ, ρ and ε, that are functions of the unknown ξ. In order to find the solution $\chi(\theta)$, it is useful to choose ξ as an intermediate variable, as it was already done for a single convection loop. Once the short-circuit function $\sigma(\xi)$ is assigned by means of Eq. (6a) or (6b), whereas function $\omega(\rho)$ is assigned by means of Eq. (14b), then the solution can be found starting from Eq. (22). This non-linear equation solved as ρ for every assigned value of ξ, gives $\rho(\xi)$. Therefore, the circulation ratio ρ is now known for every value of the dimensionless heat capacity rate ξ, and consequently, the heat exchanger effectiveness ε can be obtained from Eq. (33), or in particular from Eq. (34) or (35).

At this stage, substituting Eq. (36) in the dimensionless (19), two equations are obtained in the following form:

$$\begin{cases} \theta = \dfrac{\xi}{\xi_{th}} \cdot \dfrac{\varepsilon(\xi) + \rho(\xi) \cdot (1 - \sigma(\xi)) \cdot (1 - \varepsilon(\xi))}{\varepsilon(\xi) \cdot \left[1 - \omega\left(\rho(\xi)\right) \cdot (1 - \sigma(\xi))\right]} & \text{for} \quad \rho \leq 1 \\ \theta = \dfrac{\xi}{\xi_{th}} \cdot \dfrac{\sigma(\xi) \cdot \varepsilon(\xi) + \rho(\xi) \cdot (1 - \sigma(\xi))}{\varepsilon(\xi) \cdot \left[1 - \omega\left(\rho(\xi)\right) \cdot (1 - \sigma(\xi))\right]} & \text{for} \quad \rho \geq 1 \end{cases} \tag{37}$$

So, it is easy to determine the dimensionless operating temperature difference $\theta(\xi)$ but remarking the only values of $\xi \in [0, \xi_{th}]$ for which $\theta(\xi) \leqslant 1$ are meaningful. For every dimensionless flow thermal capacity ξ, it is then possible to evaluate χ from Eq. (20), thereby making the two functions $\theta(\xi)$ and $\chi(\xi)$, available. Finally, by eliminating the intermediate variable ξ, e.g. by means of tables or graphs, the solution $\chi(\theta)$ can be obtained. To conclude for double loop convection plant, the dimensionless solution furnishes the functions $\xi(\theta)$ and $\chi(\theta)$, as well as $\sigma(\theta)$ and $\varepsilon(\theta)$, in relation to (i) the short-circuit exponent n, (ii) the number of transfer units of the heat exchanger N, (iii) the dimensionless heat capacity rate of the cooling fluid γ, (iv) the thermodynamic limit ξ_{th} and the exponent m, if Eq. (14b) is used as the weighting function ω of the well temperature.

As was done for plant without a convection promoter, no parametric analysis of the solution is presented

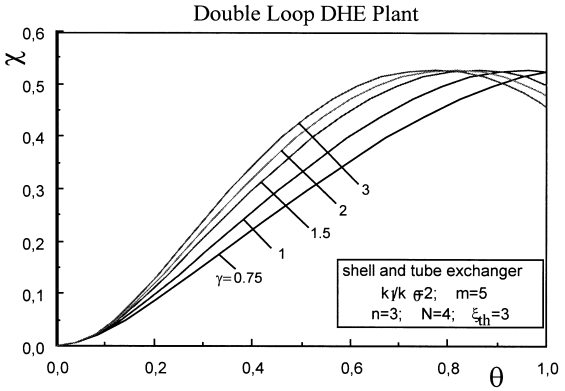

Fig. 6. Dimensionless heat flow χ vs. the dimensionless heat capacity rate of the cooling fluid γ for a DHE with convection promoter.

here, but the paper only gives the results obtained for some assigned set of model parameters, which were chosen taking into account experimental results analysis (see Section 4.2), in particular, the case of (i) a rational short-circuit function with exponent $n = 3$, (ii) a shell and tube DHE with $N = 4$ transfer units, (iii) a convection promoter with an exponent $m = 5$ of the weighting parameter ω and (iv) a circulation coefficient ratio $k_0/k_1 = 2$. Fig. 6 shows, for $\xi_{th} = 3$, that the maximum values of the dimensionless heat flow are not γ-dependent, that is, qualitatively in agreement with single loop convection results (see Fig. 4). A comparison between single and double loop convection is shown in Fig. 7, under the same aforesaid operating conditions, assuming $\gamma = 3$, and assigning two different values to the weighting parameter ω in the case of plant without a convection promoter. It is interesting to see that the convection promoter can improve performance of single loop convection plant, especially in the case of low values of the parameter ω: this improvement seems to be due to the influence of the weighting parameter ω, that in double loop convection varies, as θ increases, according to Eq. (14b).

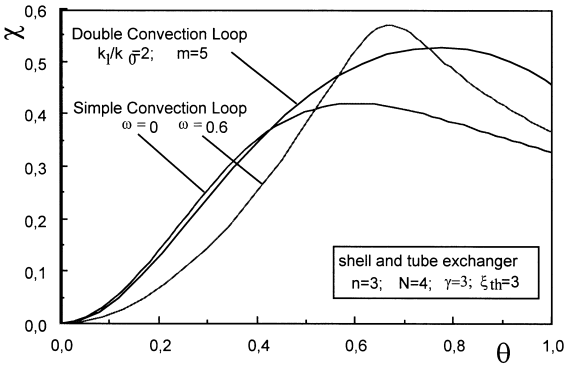

Fig. 7. Comparison between DHE with and without convection promoter vs. the weighting parameter ω.

4. Geothermal convector (GTC)

A geothermal convector (GTC) is a special application of the two-phase thermosyphon, with the evaporator placed in the well and the condenser at the ground level, and it can be considered as a particular type of DHE [4]. It was assumed, as shown in the sketch in Fig. 8, that the evaporator and the condenser operate in saturated conditions at different pressures and temperatures, so that, the two effectivenesses, one for the evaporator ε_{ev}, and the other for the condenser ε_{con}, and a thermal resistance R of the adiabatic section connecting the evaporator and condenser can be defined as [4]:

$$\varepsilon_{ev} = \frac{T_{hi} - T_{ho}}{T_{hi} - T^*_{ev}}; \quad \varepsilon_{con} = \frac{T_{uo} - T_{ui}}{T^*_{con} - T_{ui}}; \qquad R = \frac{T^*_{ev} - T^*_{con}}{\dot{Q}} \tag{38}$$

where T^*_{ev} and T^*_{con} are the mean evaporator and condenser temperatures, respectively.

The thermal resistance R is caused by the pressure difference between the evaporator and the condenser, depending on their difference in height, and on the heat flow Q transferred by the thermosyphon [1].

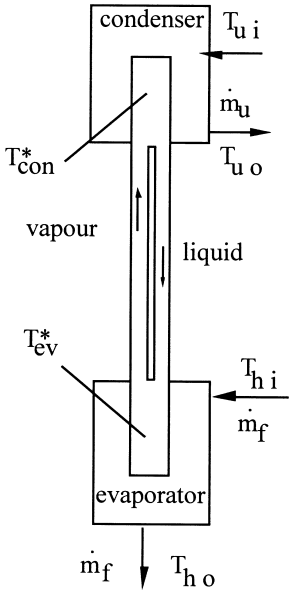

Fig. 8. Two-phase thermosyphon layout.

When the pipes connecting the evaporator to the condenser are highly thermally insulated, R can be considered as being approximately constant; but if vapour condensation is allowed inside the connecting pipes, an annular two-phase flow really occurs and R becomes a function of the heat flow, since the later is proportional to the mass flow rate of the working fluid, i.e. of the fluid circulating in the two-phase thermosyphon. In this case, a possible dependence, suggested by fitting the experimental data [8], is:

$$R = R_0 + R_1\dot{Q} + R_2\dot{Q}^2 \tag{39}$$

Assuming a phase change of the working fluid in saturated conditions at the evaporator and condenser without superheating in the vapour phase or subcooling in the liquid phase, the two effectivenesses are:

$$\begin{cases} \varepsilon_{ev} = 1 - \exp\left[-\dfrac{U_{ev}S_{ev}}{c_f\dot{m}_f} \right] \\ \varepsilon_{con} = 1 - \exp\left[\dfrac{U_{con}S_{con}}{c_u\dot{m}_u} \right] \end{cases} \tag{40}$$

This hypothesis is consistent with two-phase thermosyphon model, moreover, the effect of the vapour superheating and liquid subcooling can be considered by decreasing the heat exchanger surfaces.

In order to formulate these relationships in dimensionless form as for DHEs, it is convenient to define the transfer unit number N_{ev} and N_{con} of the evaporator and the condenser, respectively:

$$\begin{cases} N_{ev} = \dfrac{U_{ev}S_{ev}}{(c_a\dot{m}_a)_{max}} \\ N_{con} = \dfrac{U_{con}S_{con}}{(c_a\dot{m}_a)_{max}} \end{cases} \tag{41}$$

N_{ev} and N_{con}, for the sake of simplicity, can be considered as two parameters, even though the overall heat transfer coefficients U_{ev} and U_{con} are functions of the mass flow rates $\dot{m}_f$ and $\dot{m}_a$, respectively. However, the possible functional relations could be well taken into account introducing only a further complication in the model. For the adiabatic section, a dimensionless parameter λ, generally function of the dimensionless heat capacity rate ξ, can be used

$$\lambda(\xi) = R \cdot (c_a\dot{m}_a)_{max} \tag{42a}$$

In fact, introducing into Eq. (39) the dimensionless heat flow χ, which from Eq. (20) is a function of ξ, the former Eq. (39) becomes:

$$\lambda(\xi) = \lambda_0 + \lambda_1\chi(\xi) + \lambda_2\chi^2(\xi) \tag{42b}$$

Once the two-phase thermosyphon performance is completely modelled, it is possible to carry on introducing single and double loop convection, as was done for the DHE.

4.1. GTC without convection promoter

Under conditions (24) and using the aforesaid dimensionless quantities, the effectivenesses defined by Eq. (40) become:

$$\begin{aligned} &\varepsilon_{ev} = 1 - \exp(-N_{ev}/\xi); \\ &\varepsilon_{con} = 1 - \exp(-N_{con}/\gamma) \end{aligned} \tag{43}$$

These two relationships together, with the one identifying function $\lambda(\xi)$ and with the other equations of the model, supply a system of 15 equations for the unknowns T_{wo}, T_{wi}, T_{ho}, T_{hi}, T^*_{ev}, T^*_{con}, T_{uo}, $c_a\dot{m}_a$, $c_f\dot{m}_f$, σ, ε_{ev}, ε_{con}, λ, η and $\dot{Q}$.

Even though some equations of the system are nonlinear, it is possible to determine the 15 unknowns as functions of (i) the temperatures T_{ui} and T_∞, (ii) the heat capacity rate $c_u\dot{m}_u$, and (iii) the parameters $(c_a\dot{m}_a)_{max}$, n, U_{ev}, S_{ev}, U_{con}, S_{con}, R_0, R_1, R_2, k_0 and ω. It has to be remembered that the last parameter ω, in a single convection loop, is assumed to be independent of the circulating heat capacity rate. In particular, the system effectiveness η can be found as follows:

$$\eta = \left\{ \sigma(\xi) + (1-\sigma(\xi)) \cdot \left[\frac{1}{1-\exp(-N_{ev}/\xi)} + \xi\lambda(\xi) + \frac{\xi/\gamma}{1-\exp(-N_{con}/\gamma)} \right] \right\}^{-1} \tag{44}$$

In Eq. (44), it is emphasized that both, the short-circuit ratio σ and the dimensionless thermal resistance of the adiabatic section λ depend on the dimensionless heat capacity rate ξ, which is also unknown. As in the previous case of a DHE, plant performance is given through the system of Eqs. (44), (19) and (20). Once Eq. (44) is substituted in Eq. (19), it is possible to choose ξ as an intermediate variable, and consequently, to obtain:

$$\begin{cases} \theta = \dfrac{\xi}{\xi_{th}} \cdot \dfrac{\sigma(\xi) + (1-\sigma(\xi)) \cdot \left[\dfrac{1}{1-\exp(-N_{ev}/\xi)} + \xi\lambda(\xi) + \dfrac{\xi/\gamma}{1-\exp(-N_{con}/\gamma)} \right]}{1-\omega\cdot(1-\sigma(\xi))} \\ \chi = \dfrac{(1-\sigma(\xi))\left(\xi^2/\xi_{th}\right)}{(1-\sigma_{max})\left[1-\omega(1-\sigma(\xi))\right]} \end{cases} \tag{45}$$

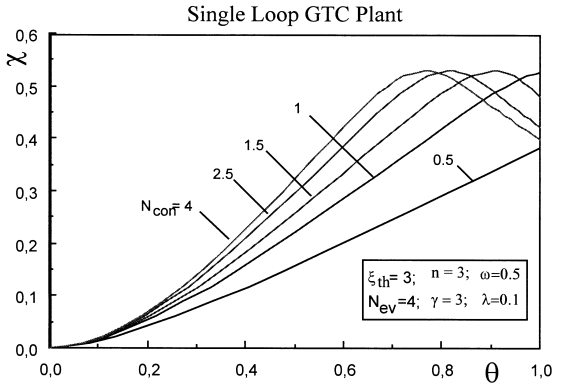

Fig. 9. Dimensionless heat flow χ vs. the dimensionless temperature difference θ as N_{con} varies for a GTC without a convection promoter with $\xi_{th} = 3$.

As for the DHE, removing the intermediate variable ξ, the functions $\xi(\theta)$, $\chi(\theta)$, and obviously $\sigma(\theta)$, $\varepsilon_{ev}(\theta)$, $\lambda(\theta)$ too, are obtained as functions of (i) the short-circuit exponent n, (ii) the two-phase thermosyphon parameters N_{ev}, N_{con} and λ_0, λ_1, and λ_2, (iii) the cooling fluid dimensionless heat capacity rate γ, (iv) the well temperature weighting parameter ω, and (v) the thermodynamic limit of heat capacity rate ξ_{th}.

By applying the aforesaid procedure, some particular cases of GTCs without a convection promoter and for a rational short-circuit function, were investigated. The results confirm the ones obtained for the single loop DHE, even if only for the cases examined; the heat flow can exhibit maximum values for dimensionless temperature differences $\theta \leq 1$. For a rational short-circuit function with exponent $n = 3$, Figs. 9 and 10 show the case of a GTC without the convection promoter

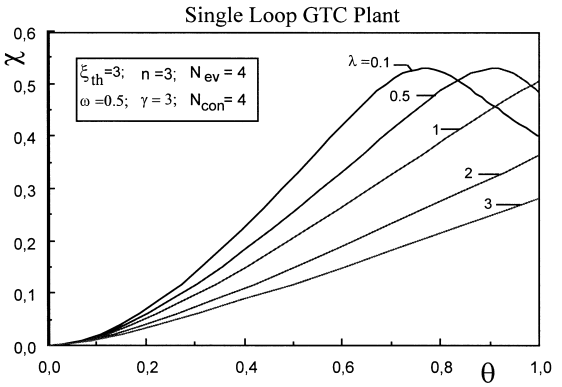

Fig. 10. Dimensionless heat flow χ vs. adiabatic section parameter λ for a GTC without a convection promoter with $\xi_{th} = 3$.

with the following parameter values $\xi_{th} = 3$, $\omega = 0.5$ and $\gamma = 3$; the reported results were obtained varying N_{con} and the dimensionless adiabatic section resistance λ, assumed as a parameter independent of heat flow.

In particular, examining the maximum points of curves concerning the dimensionless heat flow χ, it is remarkable that only the abscissa, but not the ordinate, depends on the values of the aforesaid parameters N_{con} and λ. This remark can be a matter of some importance in GTC plant operation. In fact, when non-condensable gases are present inside the condenser, the effective condensation surface and the overall heat transfer coefficient are considerably reduced, consequently, N_{con} also decreases. Furthermore, if the ascending vapour is condensed inside the adiabatic section, because of an insufficient thermal insulation of the connecting pipes, then the thermal resistance of the adiabatic section R and the corresponding parameter λ can be largely increased [8]. Nevertheless, in both cases, the maximum heat flow could be again achieved, but larger operating temperature differences would be necessary.

4.2. GTCs with convection promoter

This case is analogous to a DHE with convection promoter, and besides the dimensionless heat capacity rate ξ, it is necessary to introduce again the circulation ratio ρ. Assuming that the specific heat of the geothermal fluid is constant, $c_a \cong c_f$, the effectivenesses of the GTC evaporator and condenser are:

$$\varepsilon_{ev} = 1 - \exp\left(-\frac{N_{ev}\rho}{\xi}\right);$$
$$\varepsilon_{con} = 1 - \exp\left(-\frac{N_{con}}{\gamma}\right) \tag{46}$$

The two effectiveness equations and the parameter of the adiabatic section λ are included in the model, which for double convection loop is completed by the functional link between the parameter ω and ρ (for instance Eq. (14b)) and finally by Eq. (22). The equations are 17 in total, some of which are non-linear, and the number of unknowns is the same: T_{wo}, T_{wi}, T_{ho}, T_{hi}, T^*_{ev}, T^*_{con}, T_{uo}, $c_a\dot{m}_a$, $c_f\dot{m}_f$, ρ, σ, ω, ε_{ev}, ε_{con}, λ, η and $\dot{Q}$. These quantities can be evaluated as functions of (i) the temperatures T_{ui} and T_∞, (ii) the mass flow rate $c_u\dot{m}_u$, and (iii) the others parameters $(c_a\dot{m}_a)_{max}$, n, N_{ev}, N_{con}, λ_0, λ_1, λ_2, k_0, k_1 and m, if a function of the type (14b) is used. Naturally, since there are two validity ranges for conditions (25a) and (25b), it is necessary to make a distinction for the two intervals of ρ, obtaining for the efficiency of the system:

$$\eta = \left\{1 + \left[1 - \sigma(\xi)\right] \cdot \left[\frac{\rho(\xi)}{1 - \exp(-N_{ev}\rho/\xi)} - \rho(\xi) + \xi\lambda(\xi) + \frac{\xi/\gamma}{1 - \exp(-N_{con}/\gamma)}\right]\right\}^{-1}$$

for $\rho \leq 1$

$$\eta = \left\{\sigma(\xi) + \left[1 - \sigma(\xi)\right] \cdot \left[\frac{\rho(\xi)}{1 - \exp(-N_{ev}\rho/\xi)} + \xi\lambda(\xi) + \frac{\xi/\gamma}{1 - \exp(-N_{con}/\gamma)}\right]\right\}^{-1} \quad (47)$$

for $\rho \geq 1$

Note that, for a circulation ratio ρ equal to unity, these relationships produce Eq. (44) of a GTC without convection promoter. Furthermore, Eq. (47) contains the unknown quantities σ, ρ, and λ, and therefore, as in the previous case, it is useful to refer again to the dimensionless flow rate ξ, as an intermediate variable. Using Eqs. (6a) or (6b) for the short-circuit function $\sigma(\xi)$ and Eq. (14b) for $\omega(\rho)$, the solution of the system requires the non-linear equation (22) to be solved in relation to ρ, for every assigned value of ξ. Once the function $\rho(\xi)$ is known, Eqs. (47) are introduced into Eq. (19). Two equations are obtained, which can be written in the form:

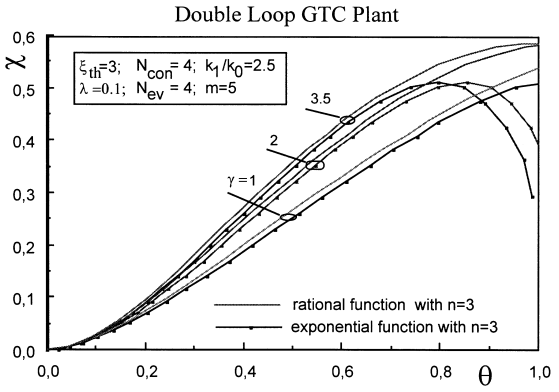

Fig. 11. Dimensionless heat flow χ vs. dimensionless temperature difference θ for a GTC with a convection promoter and rational and exponential short circuit function σ and for exponent $n = 3$.

$$\begin{cases} \theta = \dfrac{\xi}{\xi_{th}} \dfrac{1 + (1-\sigma)\left[\dfrac{\rho}{1 - \exp(-N_{ev}\rho\xi)} - \rho + \xi\lambda + \dfrac{\xi/\gamma}{1 - \exp(-N_{con}/\gamma)}\right]}{1 - \omega(1-\sigma)} & \text{for} \quad \rho \leq 1 \\ \theta = \dfrac{\xi}{\xi_{th}} \dfrac{\sigma + (1-\sigma)\left[\dfrac{\rho}{1 - \exp(-N_{ev}\rho/\xi)} + \xi\lambda + \dfrac{\xi/\gamma}{1 - \exp(-N_{con}/\gamma)}\right]}{1 - \omega(1-\sigma)} & \text{for} \quad \rho \geq 1 \end{cases} \quad (48)$$

Taking into consideration that the right-hand side, depending on functions $\sigma(\xi)$, $\rho(\xi)$, $\lambda(\xi)$ and $\omega[\rho(\xi)]$ can be calculated directly, only the dimensionless operating temperature difference $\theta(\xi)$ is left to be calculated based on the condition that $\xi \in [0, \xi_{th}]$ has to be such that $\theta(\xi) \leqslant 1$. To evaluate the heat flow it is possible to use Eq. (20), which gives the dimensionless parameter $\chi(\xi)$. The two functions obtained, $\theta(\xi)$ and $\chi(\xi)$, give the solution $\chi(\theta)$, once the intermediate variable ξ is eliminated. The elimination can be carried out by means of tables or graphs as for DHEs. To conclude, the solution is given by the dimensionless functions $\xi(\theta)$, $\chi(\theta)$, $\sigma(\theta)$, $\varepsilon_{ev}(\theta)$ and $\lambda(\theta)$, depending on: (i) the short-circuit exponent n, (ii) the transfer units of the evaporator N_{ev} and the condenser N_{con}, (iii) the dimensionless heat capacity rate of the cooling fluid γ, (iv) the thermodynamic limit of heat capacity rate ξ_{th}, and (v) the exponent m, whenever the parameter ω is assumed using Eq. (14b).

Analogous to the previous section (Section 3.1), only some results obtained for GTCs with convection promoters are given, taking into account the values suggested by the experimental analysis for the parameters (see Section 4.2). The cases examined are all identified by: (i) a thermodynamic limit $\xi_{th} = 3$, (ii) an exponent $m = 5$ of the function defining the parameter ω and (iii) an identical number of transfer units ($N_{ev} = 4$, $N_{con} = 4$) of the evaporator and condenser. For a GTC with a ratio of circulation coefficients $k_0/k_1 = 2.5$ and with a constant thermal resistance of the adiabatic section $\lambda = 0.1$, Fig. 11 compares the results obtained for short-circuit rational and exponential functions with equal short-circuit exponent $n = 3$, as γ varies. It is clear how, under the same conditions, the exponential function facilitates the existence of maximum values of the heat flow for $\theta \leq 1$. Concerning the weight of the other parameters, the results are qualitatively similar to those obtained from the analy-

sis of the GTC without a convection promoter and the DHE with a convection promoter.

The authors also examined the case of a GTC with a rational short-circuit function with exponent $n = 3$, a circulation coefficient ratio $k_0/k_1 = 3$, a dimensionless heat capacity rate of cooling fluid $\gamma = 3$, but with a function $\lambda(\xi)$ for the adiabatic section as in Eq. (42b). In order to obtain a significant comparison, some effort was made to keep the value of λ approximately equal to 0.1, when the dimensionless heat flow χ reached the maximum. In relation to this, Fig. 12 shows the influence of λ on χ, highlighting how the further non-linearity introduced into the model deforms the curve obtained for $\lambda = 0.1$; in particular, its ascending branch is inflected for low values of the dimensionless temperature difference θ.

5. Application of the model to an experimental GTC prototype

The model presented above was specially developed to provide an analytical frame for the experimental results obtained by a GTC prototype, with promoter, installed at a geothermal aquifer on the island of Ischia, Italy. The experiments were carried out over a long period of time (1989–1994) and are presented in [9]. Hence, only the information that is useful to follow how the model can be applied, is reported in the present paper.

5.1. Experimental apparatus

The working fluid of the GTC used for the experimental tests was the refrigerant R11, and the GTC components are described in detail in [4,9]. In particular, the evaporator (Fig. 13(4)) comprised 94 AISI-316 tubes with an external diameter 16 mm, a length 2.8 m, and with a resulting surface area 13.23 m^2. A high density polyethylene duct 6.16 m long with an external diameter 280 mm was used as convection promoter (Fig. 13(3)). The evaporator and the condenser, were connected by three flexible Teflon pipes (17 m long) with a metal braid reinforcement (Fig. 13(5)). In particular, two pipes with 35 mm internal diameter were used for the vapour flow, whereas for the condensate return only the one with a 16.3 mm internal diameter was used. The condenser was a common shell-and-tube heat exchanger with an overall exchange surface 6.15 m^2 (Fig. 13(6)). At the top of the condenser, two tanks with an overall volume 0.03 m^3 were installed to gather the non-condensable gases, usually dissolved in the working fluid and always released during device operation.

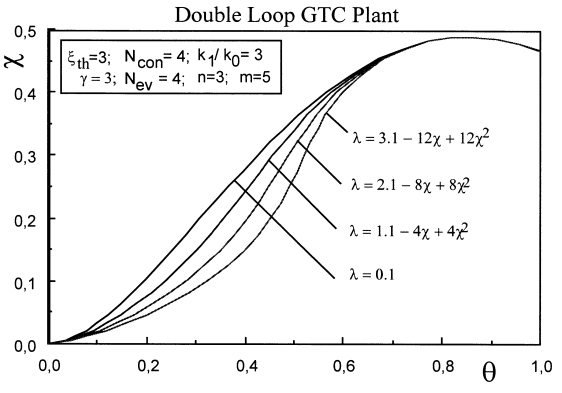

Fig. 12. Dimensionless heat flow χ vs. dimensionless temperature difference θ for a GTC with a convection promoter for different degrees of non-linear thermal resistance of the adiabatic section.

The equipment used for the GTC experimentation comprised an auxiliary apparatus and the measurement instrumentation, see Fig. 13 [9].

The cooling circuit (Fig. 13(7)) dispersed the thermal energy withdrawn from the aquifer by means of a forced draft cooling tower (Fig. 13(16)), thereby simulating thermal usage. Each test was carried out keeping constant the input temperature T_{ui}, and the mass flow rate $\dot{m}_u$, of the cooling water; its temperature at the condenser inlet was automatically regulated (Fig. 13(14), (15)), while the flow regulation was carried out manually by means of flow control micrometric valves (Fig. 13(12)). The cooling circuit was completed by some cut-off (Fig. 13(10)) and bleed valves (Fig. 13(13)) and one automatic vent (Fig. 13(9)).

The measurement instrumentation was installed partly in the cooling circuit and partly in the GTC. In particular, the following were included in the circuit (see Fig. 13): (i) a variable area flowmeter to measure the volumetric flow of the cooling water (Fig. 13(11)); (ii) two T-type thermocouples to measure the temperatures of the cooling water at the condenser input T_{ui} and output T_{uo}, respectively; (iii) a heat flow integrator to measure the total amount of heat exchanged at the condenser during long tests in order to check the two aforesaid instant measurements of the cooling mass flow and the temperature difference (Fig. 13(18)).

The GTC instrumentation comprised some T-type thermocouples to measure the temperature of the working fluid (R11) and the geothermal fluid. As regards the working fluid temperature: (i) for the condenser, two thermocouples measured the saturated vapour temperature at the condenser inlet and in the middle of the tube bank; a third thermocouple measured the condensate temperature at the condenser outlet; (ii) for the evaporator, two thermocouples

measured the temperatures of the outlet vapour and of the inlet returning fluid; another thermocouple measured the fluid temperature inside the central evaporator tube at about half the length of the tube.

As regards the geothermal fluid, the temperatures T_{hi}, T_{ho}, at the inlet and outlet of the evaporator, respectively, were measured by means of two thermocouples — the first placed at the top of the promoter, and the second placed within the promoter below the evaporator. Furthermore, it was possible to measure the geothermal fluid temperature along the annulus between the well casing and the promoter using a multi-point thermometer, i.e. four *T*-type thermocouples spaced out at 1.8 m intervals. By means of a wire and a return pulley, the multi-point thermometer can be moved along the well measuring the geothermal fluid temperature at various levels inside the annulus.

Each thermocouple of the measurement apparatus was connected to a data acquisition system, comprising a multi-channels programmable digital thermometer which recorded the measured values on a hard disk.

5.2. Analysis of the experimental results

The need for a model of the GTC system clearly arose during the tests: many of the experiments, showing unexpected plant behavior, were repeated in the attempt to attribute the experimental results to the phenomena that subsequently proved to be of only low influence. The experimental data showed that the heat flow is usually not proportional to the temperature difference between the unperturbed aquifer and the cooling water at the condenser inlet, but it reaches a maximum that does not entirely depend on the inlet temperature and the mass flow rate of the cooling water. The heat flow is a constantly rising function of the plant operating temperature difference only for low values of the mass flow rate of the cooling water. The details of the experimental data are reported in [9].

The application of the model to the analysis of the experimental data requires 14 parameters to be evaluated, most of which were not measured during the experiments. In fact, while the inlet temperature and mass flow rate of the cooling water, the temperature of the environment and of the unperturbed aquifer are measured parameters, n and m (in the case of type (14b) functions), $(c_a\dot{m}_a)_{max}$, ξ_{th}, the ratio k_1/k_0, and eventually, N_{ev}, N_{con}, R_0, R_1, R_2, are estimated in an indirect way as follows. The 10 parameters can be classified as follows: (i) parameters characterizing the aquifer and the well-promoter system, (ii) parameters identifying the heat exchangers and the operating plant

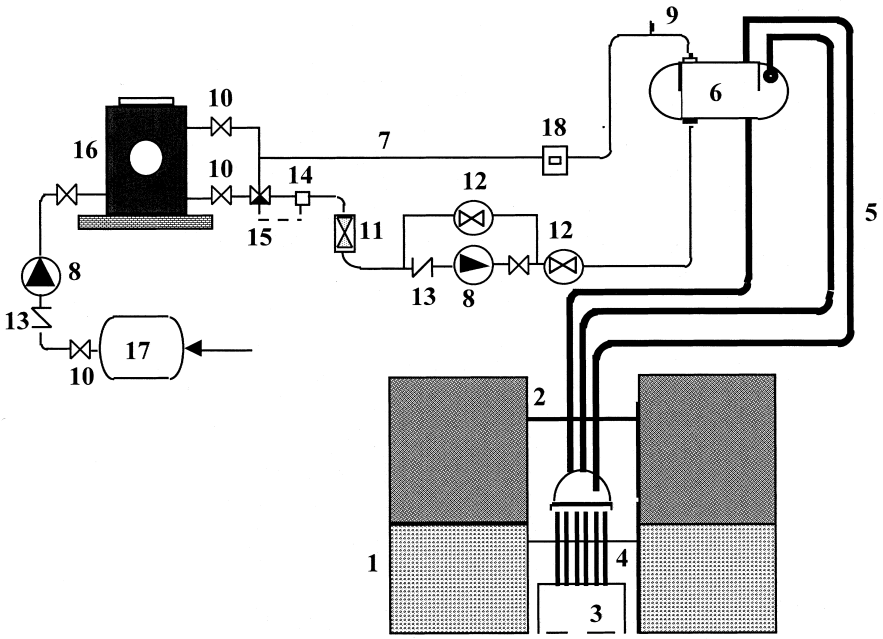

Fig. 13. Ischia plant layout: (1) geothermal aquifer, (2) well, (3) natural convection promoter, (4) GTC evaporator, (5) GTC adiabatic section, (6) GTC condenser, (7) cooling water circuit, (8) circulating pumps, (9) automatic air vent, (10) cut-off valves, (11) area variable flowmeter, (12) flow control valves, (13) check valves, (14) thermostat, (15) three-way valve, (16) cooling tower, (17) water tank, (18) calorimetric flowmeter.

conditions. According to the model presented here, the former have to be considered independent of the latter, that is independent of the operating conditions. On account of this hypothesis, the measurements had to be carried out in steady state conditions. During the experiments, a strict steady state was not always possible because the transient in the heat exchangers and the well-aquifer system had very different response times (from a few hours to some days), and also some aquifer perturbations arose, not for natural reasons, but as results of the mass flow rates withdrawn by neighboring active wells. Therefore, together with the inevitable uncertainty of the measurements, the unsteady state has to be considered the main cause of dispersion of experimental data.

Assuming there to be an aquifer steady state, for short circuit σ and the weighting parameter ω rational functions were chosen. The parameters n and $(c_a\dot{m}_a)_{max}$ were estimated from the numerical simulations of the Ischia aquifer. These simulations, reported in [9], determined a value of n close to 3 and showed that $(c_a\dot{m}_a)_{max}$ is only function of aquifer properties, and therefore independent of heat flow. For Ischia aquifer, the range is $2.0 \leq (c_a\dot{m}_a)_{max} \leq 2.3$ kW/°C.

For the Ischia plant, from the well temperature trends [4,9] measured during the experiments, m is estimated to be comprised in the range $3 \leq m \leq 7$ with a mean value close to 5.

The k_1/k_0 values can be estimated from momentum equations balance and density differences of geothermal fluid, taking into account temperature measurements in the well and aquifer. For the Ischia plant, results showed values in the range $1.2 \leq k_1/k_0 \leq 3.5$.

From estimates of k_0 and $(c_a\dot{m}_a)_{max}$ and from measurements of T_∞ and T_e, a constant value of ξ_{th} close to 4 can be determined using Eq. (18).

Other parameters characterizing the device were selected on the basis of the plant's actual operating conditions. With regards to the overall heat transfer coefficients of GTC components, at the evaporator the film control coefficient was due to the geothermal fluid convection outside the evaporator tubes, whereas at the condenser it was due to the cooling water convection inside the tubes. In particular, because of the range of the cooling mass flow rate used, inside the condenser tubes there was mixed laminar convection and the heat transfer coefficient was a function of the Graetz number, and, consequently, of the cooling mass flow rate [10]. Outside the evaporator tubes mixed convection also occurred, but the situation of the geothermal fluid flow was more complex, owing to the geometry and the type of convection induced by the convection promoter.

On the basis of these considerations, for a volumetric flow rate of the cooling water of 3 m^3/h, the authors determined an overall heat transfer coefficient of about 380 W/m^2 K for the evaporator and 400 W/m^2 K for the condenser using heat transfer correlations [10] consistent with the experimental data. Hence, from estimate of $(c_a\dot{m}_a)_{max}$, the numbers of transfer units, N_{ev} and N_{con}, can be estimated using Eq. (27), obtaining practically constant values equal to 2.5 and 1.25, respectively. For the adiabatic section thermal resistance, the coefficients of Eq. (39) were estimated on the basis of the experimental tests [9]. These coefficients correspond to a temperature drop between evaporator and condenser of about 5 K at 10 kW and 2 K at 20 kW. The reduction of the adiabatic section resistance raising of the heat flow is in qualitative agreement with the pressure drop of the two-phase flow occurring inside the connecting pipes with not perfectly insulated walls. In particular, as the heat flow and, consequently, the vapour mass rate and velocity are increasing, all the patterns of the countercurrent and cocurrent vertical annular flow can occur inside the vapour ducts.

Table 1 gives the fitting parameter values used for double loop GTC model. In particular, measured temperature of the unperturbed aquifer and estimated exponents of the functions mentioned, together with the other estimated parameter values characterizing the aquifer, the well-promoter system and the device, are reported. Moreover, the lowest temperature of the cooling water, reported in Table 1 as the environmental temperature, was that achieved by the plant cooling tower [9].

Finally, Fig. 14 reports both, the experimental results and the fitting curve evaluated using the double loop GTC model, for 3 m^3/h of cooling water. The excellent results obtained are due not only to the great number of degrees of freedom available, but also to the ability of the model. In fact, the values of the 10 parameters not measured are contemporary included in the ranges estimated and obtained with different

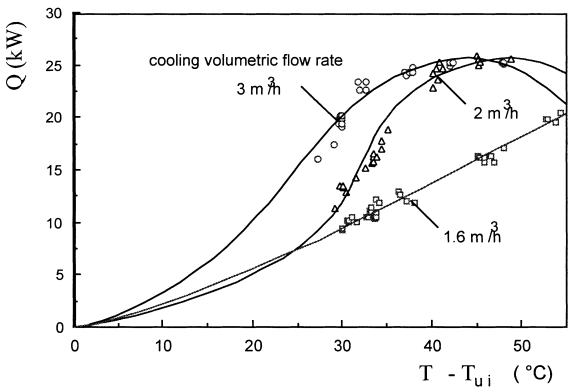

Fig. 14. Application of the model of GTC with a convection promoter to the experimental results [9].

Table 1
Fitting parameters values

Cooling water volumetric flow rate (m^3/h)	3	2	1.6
Cooling water heat capacity rate, $c_u\dot{m}_u$ (kW/K)	3.47	2.32	1.85
Unperturbed aquifer temperature, T_∞ (K)	73.3	73.3	73.3
External ambient temperature, T_e (K)	19	19	19
Geothermal fluid maximum heat capacity, $(c_a\dot{m}_a)_{max}$ (kW/K)	2	2	2
Dimensionless heat capacity rate thermodynamic limit, ξ_{th}	4	4	4
Short circuit rational exponent, n	3	3	3
Thermal weighting parameter, ω function exponent, m	5	5	5
Circulation coefficients ratio, k_1/k_0	3.5	3.5	1.25
Evaporator unit transfer number, N_{ev}	2.5	2.5	1
Condenser unit transfer number, N_{con}	1.25	1	0.7
First adiabatic section coefficient, R_0 (K/kW)	1.25563	3.06408	1.50423
Second coefficient of adiabatic section, R_1 (K/kW^2)	−0.096451	−0.241127	−0.072234
Third coefficient of adiabatic section, R_2 (K/kW^3)	0.001929	0.048225	0.001447

approaches (numerical simulations, momentum and energy balace equations, heat transfer correlations, etc.). Clearly, a sensitivity analysis on the parameters choice was developed by the authors, but its presentation in this paper is not allowed because of the high number of the parameters. However, the results of sensitivity analysis are similar to those shown in Fig. 3–Fig. 12. In fact, several parameters used in these figures are the same used for the fitting curve of the experimental results of the Ischia plant.

For the case concerning 2 m^3/h of cooling water, the parameters in Table 1 were assumed. Compared to the previous case, the situation did not change at the evaporator, whereas at the condenser the overall heat transfer coefficient decreased from 400 to 325 W/m^2 K, due to a 30% reduction in the cooling water flow rate. For the thermal resistance of the adiabatic section, the fitting of the experimental data required coefficients corresponding to a temperature drop of about 5 K at 25 kW. The increase in resistance of the adiabatic section can be explained as an unexpected change in the geometry of the flexible connecting tubes: an inspection after a long working period revealed some pipe supports had collapsed inside the well, to form an anomalous curve where some condensed liquid could have gathered. Probably this arose during the GTC tests carried out for 2 m^3/h of cooling water. The interpolation results are still very satisfactory, as shown in Fig. 14.

This figure also shows the results obtained for a volumetric flow rate of cooling water equal to 1.6 m^3/h, with the convection promoter shortened by 70 cm. This reduction was necessary to avoid a recurrent phenomenon: a shifting of the geothermal fluid level in the well periodically disconnected the secondary convection loop in the well, preventing the GTC from reaching steady state conditions [9]. Therefore, the convection promoter was cut, even though it was always clear that this operation would cause a decrease in the driving forces, a consequent drop of the geothermal fluid flow through the promoter and the evaporator tube bundle, and eventually a deterioration in plant performance [9]. The mass rate reduction of the fluid flow circulating in the promoter was estimated as circa one-third of the previous value; hence, the ratio of the circulation coefficients was reduced, and, finally, for the evaporator an overall heat transfer coefficient decrease to 150 W/m^2 K was calculated. The corresponding parameters are presented in Table 1. The remaining values of Table 1 concerning the 1.6 m^3/h volumetric flow rate were suggested by fitting the experimental data. The thermal resistance of the adiabatic section corresponds to a temperature drop of 9 K at 10 kW, which could be still explained by means of the aforementioned formation of the anomalous U-bend in the connecting pipes; whereas an overall heat transfer coefficient of about 225 W/m^2 K (not completely justified for a cooling flow rate of 1.6 m^3/h) would correspond to the condenser at the value assumed by N_{con}. More probable estimations give an overall heat transfer coefficient of about 300 W/m^2 K, which requires a condenser surface of just 4.67 m^2 compared to 6.15 m^2 calculated by geometry. This inconsistency is probably due to two concomitant reasons. The first is the possible presence of non-condensable gases inside the condenser shell, which, having completely filled the two gathering tanks, make part of the condenser surface inoperative. The second is a presence of air dissolved in the cooling water flowing in the condenser tubes, despite the automatic air valves installed in the plant. The mixing between water and air continuously occurred in the cooling tower, and then the

water flow released some air in different parts of the circuit. Especially for small values of water mass flow rate, the released air was not washed away, but gathered in several zones, and this would happen in the upper part of the condenser head cover [9]. It was sufficient for air to obstruct about 10 of the tubes in the upper part of the tubesheet, to bring about the necessary reduction of the overall heat transfer coefficient.

6. Conclusions

In this paper, the authors have completed the lumped parameters model of the phenomena that cause heat flow limits in one-well geothermal plants. The model was developed and extended to both single and double loop natural convection plant with the heat exchanger placed at the bottom of the well. In particular, besides plant with DHEs which uses traditional heat exchangers, plant with GTCs was also studied since, in previous years the authors had the opportunity to experimentally investigate a GTC plant prototype on site.

The model, which was formulated in dimensionless terms in order to facilitate a parametric study, illustrates plant performance and allows one to show that, for suitable values of the parameters, there are limitations to the maximum heat flow transferred. The model was also applied to the data fitting of the experimental results available to the authors. The excellent results obtained are due not only to the great number of degrees of freedom available, but also to the ability of the model, even if with some simplifications, to take into account the main thermal and fluid-dynamic phenomena that define the performance of one-well geothermal fluid circulation plant.

References

[1] A. Carotenuto, C. Casarosa, M. Dell'Isola, L. Martorano, An aquifer–well thermal and fluid dynamic model for downhole heat exchangers with a natural convection promoter, Int. J. Heat Mass Transfer 40 (18) (1997) 4461–4472.

[2] A. Carotenuto, C. Casarosa, Modello a Parametri Concentrati dei Limiti Operativi di Impianti Geotermici a Pozzo Unico. Parte I: Elementi Generali, 53°Congresso Nazionale ATI, Firenze, vol. I, 1998, pp. 557–570.

[3] K.D. Rafferty, G. Culver, Heat exchangers, Geo-Heat Center Bulletin 19 (1) (1998) 20–26.

[4] E. Latrofa, C. Casarosa, L. Martorano, M. Cannaviello, A. Carotenuto, Geothermal convector design: solution, design criteria, calculation methods, Energy Sources 16 (1994) 531–547.

[5] R.G. Allis, R.C. James, A natural convection promoter for geothermal wells, Geothermal Resources Council Transaction 4 (1980) 409–412.

[6] G. Buonanno, A. Carotenuto, C. Casarosa, L. Martorano, Aquifer–well thermal and fluid dynamic model to design a downhole heat exchanger, Journal of Porous Media I (2) (1998) 167–180.

[7] A.F. Mills, Heat Transfer, in: Irwin, Homewood, IL, 1992, pp. 730–735 (Chap. 8).

[8] C. Casarosa, F Fantozzi, E. Latrofa, Individuazione e superamento dei limiti termofluidodinamici interni di un termosifone bifase per impieghi geotermici, in: Proc. of Seminario Informativo Attività di ricerca del Sottoprog. Energia Geotermica, SI-5, 639, Ediz. PFE, Roma, 1988.

[9] A. Carotenuto, C. Casarosa, L. Martorano, The geothermal convector experimental and numerical results, Applied Thermal Engineering 19 (4) (1999) 349–374.

[10] Rohsenow W.M., Hartnett J.P., Ganic E.N (Eds.), Handbook of Heat Transfer Fundamentals, 2nd ed., McGraw-Hill, New York, 1985 (Chap. 6), pp. 76–78; (Chap. 7), pp. 106–111.